Energy Conversion and Management 155 (2018) 128–137

Contents lists available at ScienceDirect

Energy Conversion and Management

journal homepage: www.elsevier.com/locate/enconman

Biodiesel production by valorizing waste *Phoenix dactylifera* L. Kernel oil in the presence of synthesized heterogeneous metallic oxide catalyst (Mn@MgO-ZrO_2)

Farrukh Jamil[a], Ala'a H. Al-Muhatseb[a,*], Myo Tay Zar Myint[b], Mohab Al-Hinai[c], Lamya Al-Haj[c], Mahad Baawain[d], Mohammed Al-Abri[a], Gopalakrishnan Kumar[e], A.E. Atabani[f]

[a] Department of Petroleum and Chemical Engineering, College of Engineering, Sultan Qaboos University, Muscat, Oman
[b] Department of Physics, College of Science, Sultan Qaboos University, Muscat, Oman
[c] Department of Biology, College of Science, Sultan Qaboos University, Muscat, Oman
[d] Department of Civil and Architectural Engineering, College of Engineering, Sultan Qaboos University, Muscat, Oman
[e] Department of Environmental Engineering, Daegu University, Republic of Korea
[f] Energy Division, Department of Mechanical Engineering, Faculty of Engineering, Erciyes 20 University, 38039 Kayseri, Turkey

ARTICLE INFO

Keywords:
Biodiesel
Waste *Phoenix dactylifera* L. kernel oil
Heterogeneous metallic oxide catalyst
Transesterification
Esterification

ABSTRACT

The present study intended to produce biodiesel as an efficient fuel from waste *Phoenix dactylifera* L. kernel oil in the presence of synthesized efficient heterogeneous metallic oxide catalyst (Mn@MgO-ZrO_2). The performance of synthesized metallic oxide catalyst was evaluated based on biodiesel yield and the process has been optimized. The optimum biodiesel yield was 96.4%, when process temperature was 90 °C, catalyst loading 3 wt%, methanol to oil ratio 15:1 and reaction duration was 4 h. The product biodiesel was characterized in order to evaluate its quality according to ASTM and EN standards. Thus, characterization of biodiesel revealed that it fulfills the standard ranges defined by ASTM and EN: its acid value was 0.11 mg KOH/g, density 881 kg/m^3, viscosity 3.85 mm^2/s, flash point 142 °C and suitable low-temperature properties. It can thus be concluded that synthesized heterogeneous catalyst can be used efficiently for biodiesel production from waste *Phoenix dactylifera* L. kernel oil which satisfied the international standards defined by ASTM and EN.

1. Introduction

Currently, large-scale production of biodiesel relies on edible oils, which entails high production costs, as up to 70% of the cost is attributed to feedstock [1,2]. Several kinds of vegetable oils have been used for the production of biodiesel, which includes canola, palm, palm kernel, sunflower and coconut oil; but the major issue regarding the consumption of these oils is the high cost of the final form of combustible vegetable oil, as compared to fossil diesel. It also causes food *versus* fuel controversy [3,4]. Present and future research are/will be focused on important issues regarding biodiesel production from low cost, non-edible and waste biomass sources, which tend to reduce biodiesel cost, environmental issues and emission of toxic gases [5].*Phoenix dactylifera* L. is known to be a flowering plant species of the palm family and is the most common agricultural product in Middle Eastern and North African countries [6,7]. Of all the producers of *Phoenix dactylifera* L. worldwide, Oman is the ninth largest [8]. The fruit consists of nutritious fleshy pericarp and pit, which weighs 10–15% of the total fruit. Meanwhile, the industries processing *Phoenix dactylifera* L. for different purposes consider pits as waste and the same are either dumped or used for animal feed [9]. However, oil extracted from pits is considered to be a high-value product with unsaturated fatty acids (54.85%) and saturated fatty acids (45.14%) with low kinematic viscosity [9,10]. The fatty acid profile of pits oil is: lauric acid (16.44%), myristic acid (9.96), palmitic acid (9.54%), stearic acid (2.38%), oleic acid (55.36%) and linoleic acid (6.32%), which is almost similar to the majority of vegetable oils used for biodiesel production [11,12]. Moreover, biodiesel synthesized from *Phoenix dactylifera* L. pits oil revealed potential fuel properties which are according to international standards (EN and ASTM) set for biodiesel [13].

Biodiesel synthesis using heterogeneous catalysis is a promising technique, as it involves less number of unit operations, non-corrosive and environmentally friendly, facile catalyst product separation, less number of disposal issues and their recyclability and reusability [14–19]. Basic heterogeneous catalysts are widely used for biodiesel synthesis; but their intrinsic property of sensitivity towards high free

* Corresponding author.
E-mail address: muhtaseb@squ.edu.om (A.H. Al-Muhatseb).

http://dx.doi.org/10.1016/j.enconman.2017.10.064
Received 25 August 2017; Received in revised form 16 October 2017; Accepted 22 October 2017
0196-8904/ © 2017 Elsevier Ltd. All rights reserved.

fatty acids (FFA) oil, tends to form soap and problems are encountered in phase separation of triglyceride and glycerol [20–24]. While acidic heterogeneous catalysts are not sensitive to high FFA oils [25] and are capable of catalyzing the unrefined and low-cost oils without any pre-treatment, water present or generated during esterification can transform the triglycerides by hydrolysis into diglycerides, which form more FFA and also cause leaching and deactivation of catalysts [26–29].

In order to overcome issues related to heterogeneous acidic and basic catalysts, a new catalyst with tailored characteristics of solid acidic catalysts to tackle FFA oil and solid basic catalysts for efficient transesterification of triglycerides are considered [30]. The basic characteristic of a bi-functional catalyst is that in its presence, both esterification and transesterification occur simultaneously [31]. Moreover, the effect of high FFA and water contents can be nullified by adjusting the properties of bi-functional catalysts. Therefore, for efficient bi-functional catalysts, the support material should be amphoteric in nature, modified by active acidic or basic promotors. Zirconium oxides, based on their amphoteric nature, have been reported to be efficient base material, which can be modified depending on desired physiochemical properties for the type of oil being processed. Earlier, zirconium oxides have been modified in both routes such as in acidic forms SO_4^{2-}/ZrO_2, TiO_2/ZrO_2, Al_2O_3/ZrO_2, sulphated zirconium-aluminum (SZA) and tungstate zirconia-alumina (WZA) and in basic forms modified by KOH, MgO, CaO and La_2O_3 [32–34]. Thus zirconium modified forms to achieve desired characteristics of the catalyst can be considered.

In the present study, waste *Phoenix dactylifera* L. oil was valorized to produce biodiesel. The biodiesel was produced in presence of a synthesized efficient heterogeneous metallic oxide catalyst (Mn@MgO-ZrO_2). Detailed, characterization of the synthesized catalyst was done by several analytical techniques to determine its nature. The process parameters for biodiesel production which include; temperature, time, catalyst loading and methanol to oil ratio were optimized. Thus this study can contribute additional inputs for biodiesel production, using a metallic oxide catalyst which possesses both acidic and basic sites to produce high-quality biodiesel.

2. Experimental

2.1. Materials

Phoenix dactylifera L. kernels were purchased from a local company in Muscat, Oman. The kernel oil was extracted by using *n*-hexane as solvent and soxhlet device according to AOCS official method Am 2–93. Zirconium oxide, potassium hydroxide, potassium bicarbonate, methanol, and *n*-hexane were purchased from Aldrich. Meanwhile, magnesium nitrate hexahydrate and manganese nitrate tetrahydrate were purchased from Merck. Analytical reagent grades were applied throughout this research work.

2.2. Catalyst preparation

Preparation of heterogeneous metallic oxide catalysts involved the following steps. First MgO-ZrO_2 support was prepared by varying the ratio Mg:Zr from 0.2 to 0.5 by conventional co-precipitation method. A homogenous precursor solution for support was formed in 100 ml of distilled water and an aqueous solution (of 1 M KOH and 0.25 M K_2CO_3) was added dropwise into the solution, to maintain the pH 10 of the solution, followed by continuous stirring for 2 h. The complete solution was left for 24 h and subsequent filtration and washing of the precipitate was done, till it was neutralized. The material then dried overnight in an oven at 120 °C and was calcined in a muffle furnace at 650 °C (Suppl. Fig. S1) for 4 h with a ramping rate of 4 °C/min. Modification of support material MgO-ZrO_2 involved the impregnation of metal (Mn) by incipient wetness impregnation. The support was impregnated with an aqueous solution of manganese nitrate tetrahydrate to obtain 4 wt% of Mn metal on MgO-ZrO_2. After impregnation, the resultant material was dried in an oven at 100 °C overnight, followed by calcination at 650 °C for 4 h with the linear heating rate of 4 °C/min.

2.3. Catalyst characterization

X-ray powder diffraction (XRD) patterns were measured on PANalytical, Xpert PRO instrument, USA, equipped with rotating anode and Cu Kα radiation. The measurements were conducted in continuous θ/2θ scan refraction mode. Scanning electron microscope (SEM: JEOL JSM-7800F, Japan) images and energy dispersive X-ray spectroscopy (EDXS) spectra were recorded to obtain particle morphology and elemental analysis. Transmission electron microscope (TEM: JEOL, JSM-2100F, Japan) images and respective EXDS spectra were recorded for crystal morphology and elemental analysis, which was operated at 200 kV and equipped with a microprobe system. Thermogravimetric analysis TGA was performed using the simultaneous thermal analyzer STA 6000 Perkin Elmer. Initially, 10 mg sample material was heated from ambient temperature to 900 °C with a heating rate of 10 °C/min in the inert atmosphere of nitrogen gas flowing at the rate of 40 ml/min. The BET surface area, pore size, and pore volume measurements were carried out using a standard adsorption equipment (ASAP 2020, Micromeritics Instruments Inc., Norcross, GA, USA) using N_2 gas (99.995% pure). X-ray photoelectron spectroscopy (XPS) spectra's were attained using multi-probe XPS (Omicron Nanotechnology, Germany) with a monochromatic Al Kα radiation ($h\nu$ = 1486.6 eV) working at 15 kV, 20 mA. During measurement, the sample surface was flooded with electron using neutralizer (CN 10, Omicron Nanotechnology, Germany). The presence of acidic and basic sites in the catalysts was detected by temperature programmed desorption (CO_2 & NH_3- TPD) with Thermo Finnigan TPDRO 1100 Series instrument. About 0.5 g of sample was taken in inner tube quartz reactor and covered with quartz wool. For TPD, the sample was pre-treated by passing a continuous flow of nitrogen gas and simultaneously, the sample was heated from 50 to 150 °C for 60 min, in order to remove any moisture present in the sample. Then, for adsorption of NH_3 or CO_2 in the sample, it was flushed with a continuous supply for 60 min at ambient temperature and before the analysis; the sample was pre-treated again in order to remove any excess NH_3 or CO_2, by passing nitrogen gas with 20 ml/min. through the sample for 60 min at ambient temperature. Then, the sample was heated to 950 °C from 50 °C at the heating rate of 10 °C/min, while helium was used as carrier gas with 20 ml/min. Desorption of NH_3 and CO_2 from samples was done by thermocouple detector and the intensity of gas *versus* temperature was plotted.

2.4. Methanolysis of Phoenix dactylifera L. Kernel oil and quality analysis of biodiesel

Methanolysis was carried out in a system consisting of a hot plate with a temperature controller and rpm controller mechanical stirrer, three neck flat bottom flask and reflux condenser. The process parameters were varied within the defined ranges as mentioned in Table 1. Oil with constant stirring was heated initially up to the desired temperature. Once the temperature was attained, the desired amount of catalyst and methanol were added to the vessel. The reaction was run

Table 1
Process parameters along with their ranges used for biodiesel production by transesterification.

	Parameter	Low	High
1	Temperature (°C)	60	100
2	Methanol to oil molar ratio	7.5	37.5
3	Catalyst (wt%)	1.5	7.5
4	Time (h)	1	5

for the required time and then the catalyst from the liquid product was centrifuged, filtered and poured into the separating funnel, to separate the biodiesel from glycerol. The product biodiesel was washed thoroughly with warm water to remove impurities completely. Further on, a rotary evaporator was used to remove any water or methanol which was still present in the produced biodiesel. In the end, a small amount of sodium sulphate beads were added to remove the moisture completely from biodiesel. Biodiesel composition was determined by a Perkin Elmer Clarus 600 gas chromatograph mass spectrometer (GC–MS), using a DB-Wax column. Helium was used as a carrier gas with a constant flow of 1.0 ml/min, with a 1 µl sample injected with mass spectrometer set to a scan a frequency range of 40–550 amu. The initial oven temperature was set to 80 °C and held for 5 min, before being increased to 240 °C at a heating rate of 4 °C/min. Quality of the synthesized biodiesel was evaluated based on its fuel properties determined according to European standards-EU and Analytical standard testing materials ASTM methods. The determined fuel properties involve density (ASTM 5002), cetane number (ASTM D613), cloud point (ASTM D2500), cold filter plugging point (ASTM D6371), pour point (ASTM D97), kinematic viscosity (ASTM D445), flash point (ASTM D93) and acid value (ASTM D664). Each test was repeated three times in order to achieve accurate data.

$$Yield = \frac{weight\ of\ biodiesel}{weight\ of\ oil} \times 100\%$$

3. Results and discussions

3.1. Catalyst characterization

The XRD patterns for pristine ZrO_2 and along with different loading of MgO are shown in Fig. 1. It can be observed that the presence of MgO at 42.10° for different MgO loadings samples and remaining all other peaks are characteristic peaks for ZrO_2 (pattern a). Moreover, the crystal structure of ZrO_2 was initially monoclinic, which was confirmed by intense peaks present at 28.1° and 31.6° respectively. After loading of MgO and calcination, similar kind of patterns was observed (pattern b, c, d, and e) with additional peaks of loaded alkaline earth metal (Mg), which indicates that it sustained its crystal structure.

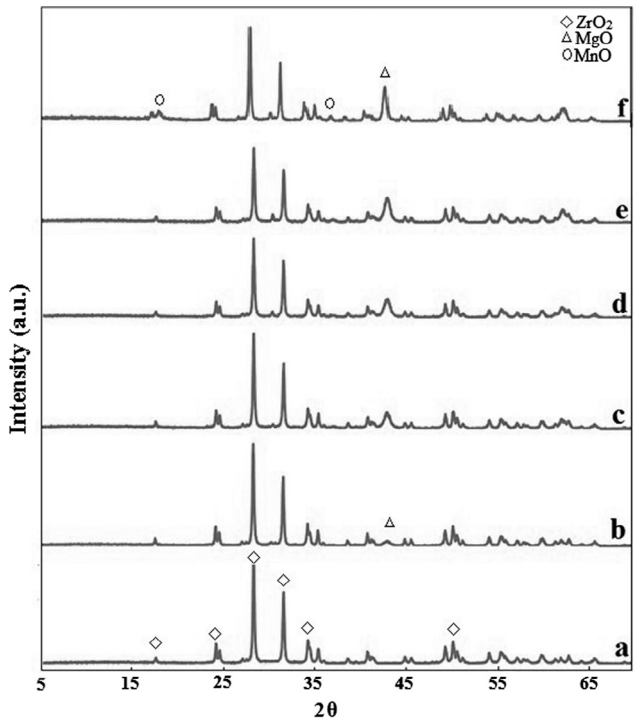


Fig. 1. XRD patterns of synthesized heterogeneous catalysts for biodiesel production. (a) for ZrO_2 (b–e) for catalysts modified by variation Mg:Zr (0.2–0.5) and (e) represents the best combination (0.4Mg:Zr) with respect to biodiesel yield and further modified by manganese (Mn).

Meanwhile, it can be depicted that when the amount of MgO loading has been increased, the intensity of MgO peak increased, which can be attributed to the fact that initially, MgO formed mixed oxide form of zirconium oxide and magnesium oxide; and as the amount of MgO is increased, it becomes prominent at 42.10° and the small peak at 30.7° represents the presence of mixed oxides (MgO-ZrO_2). Similar kind of pattern has been reported by Renuka et al. for MgO doped with zirconium oxide, in which they observed that by increasing the amount of MgO on the based material, the crystalline nature of zirconium oxide was maintained [35]. Besides this, in Fig. 1, pattern f represents MgO-ZrO_2 modified further with MnO and the peaks present at 17.61° and 36.22° show the presence of Mn in the material. Hence, based on the observed pattern of XRD and the presence of peaks representing Mg and Mn in ZrO_2 structure, it can be attributed to the successful synthesis of metallic oxide catalysts. Moreover, based on XRD data and by using Scherrer equation the crystal size has been determined for each metal oxide (Zr = 39 nm, Mg = 32 nm, and Mn = 18 nm).

The internal morphology was analyzed by TEM and elemental mapping was also obtained to determine the particle distribution as a function of the position of the sample. The TEM images for each catalyst which contains the BF image of each sample along with each element present in the sample, are shown in Fig. 2(a–e). It can be observed from images that each of the materials is well dispersed and from the BF images and even from TEM micrographs, that each catalyst possesses definite crystal structure. Elemental mapping confirmed the presence of each metal on the parent ZrO_2. The results from TEM and elemental mapping were in good agreement with SEM and EDX analysis (Suppl. Fig. S2), which showed the good dispersion of impregnated metals along with their definite presence.

The surface analysis for synthesized catalysts was carried out by X-ray photoelectron spectroscopy XPS. To obtain the structural differences while changing MgO concentration on the base material, XPS analyses are used. Fig. 3 shows the XPS spectra of all samples in O1s binding energy. It can be seen that pure ZrO_2 exhibits the peak at a binding energy of 530.0 eV and by increasing the amount of the MgO on ZrO_2, the peak starts shifting from 530.0 eV towards the peak of pure MgO at a binding energy of 531.0. The increment of binding energy in MgO-ZrO_2 composite can be related to the strong interaction between the two. Metal support interaction has a large influence on the average valence oxidation states of different elements in the catalyst. It has been reported that metals with higher oxidation state have higher binding energy, as compared to that present in lower oxidation state [36]. Further, it can attribute that by changing the composition and adding more components in the catalysts changes the interaction strength, chemical environment of the material and binding energy [37]. So, these results are in agreement with the physiochemical properties of catalysts which also indicate the strong interaction between MgO-ZrO_2.

Moreover, XPS full spectra of MgO-ZrO_2 impregnated with Mn is shown in Fig. 4. The spectra reveal the presence of all components such as Mg, Zr, O, and Mn in synthesized metallic oxide catalyst. The high-resolution spectra for Mn 2p (Fig. 4: Inset) show that the Mn $2p_{3/2}$ has the binding energy of 640.6 eV, while Mn $2p_{1/2}$ has a binding energy of 651.2 eV, with the spin energy separation between the two of 10.6 eV. The reported results are in good agreement with literature reported earlier for MnO_2 [38].

Temperature programmed desorption (TPD) has been carried out with CO_2 and NH_3 adsorption-desorption for measuring the basic and acid character of catalysts. The CO_2-TPD patterns for ZrO_2, along with all its modified forms, are shown in Fig. 5. CO_2-TPD can detect the active sites in materials of different basic strength such as weak basic sites, which occurs due to bicarbonates, moderate basic sites which are normally due to the presence of bidentate carbonates and strong basic

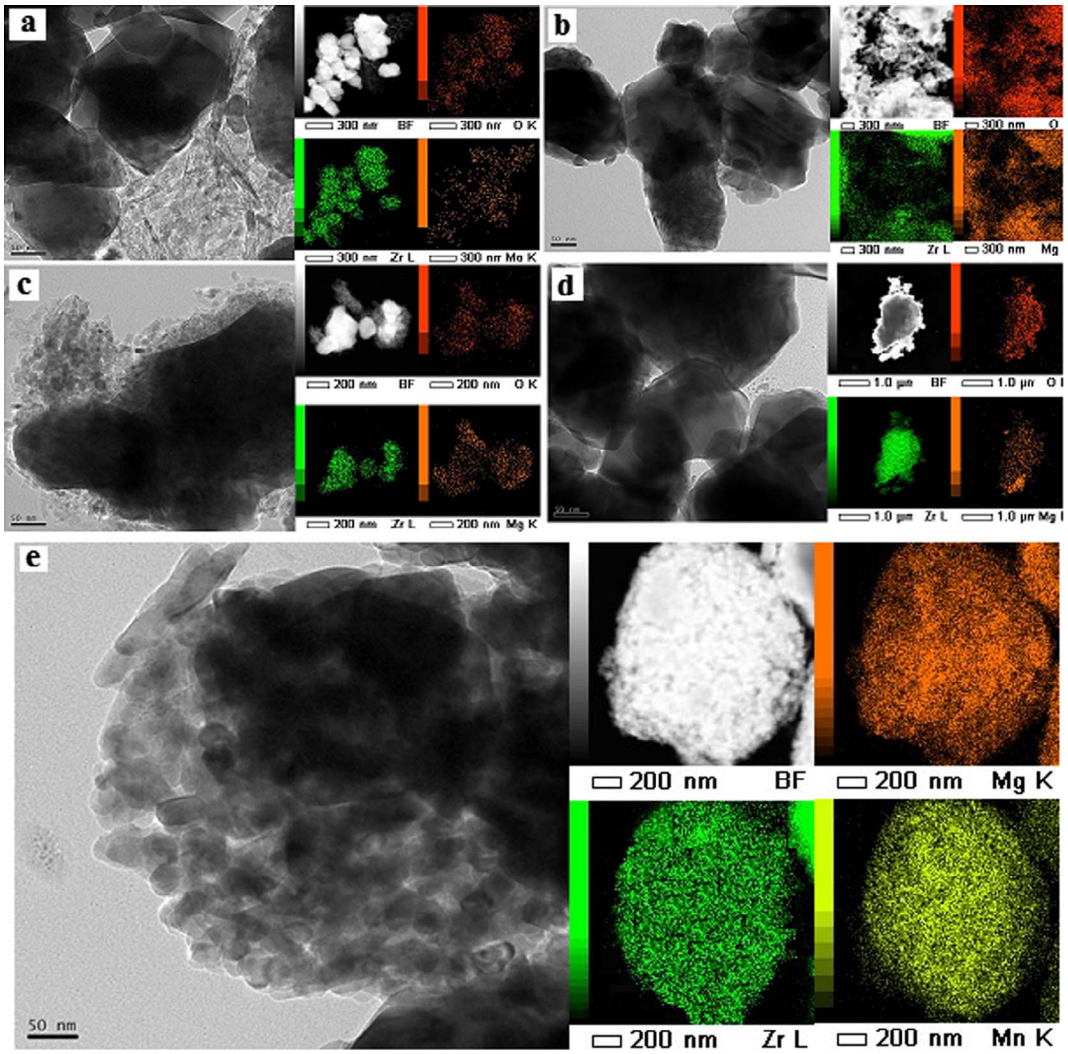


Fig. 2. TEM images of synthesized catalysts along with the elemental mapping; images (a–d) for 0.2–0.5 Mg:Zr along with elemental mapping showing the presence of all elemental and image (e) for 0.4 Mg:Zr along with its elemental mapping modified with Mn.

sites, which are shown due to the presence of monodentate [39]. It can be observed from Fig. 5 that pure ZrO_2 shows the presence of a single peak at 120 °C, which can be referred to weak basic sites on the surface of the material. However, when MgO is added to the substrate, it can be observed that there are three peaks present in the pattern, which refers to the presence of basic sites with different strengths. The peaks appearing from 100 to 220 °C can be ascribed to the presence of weak basic sites, while peaks from 220 to 370 °C and 370 to 620 can be

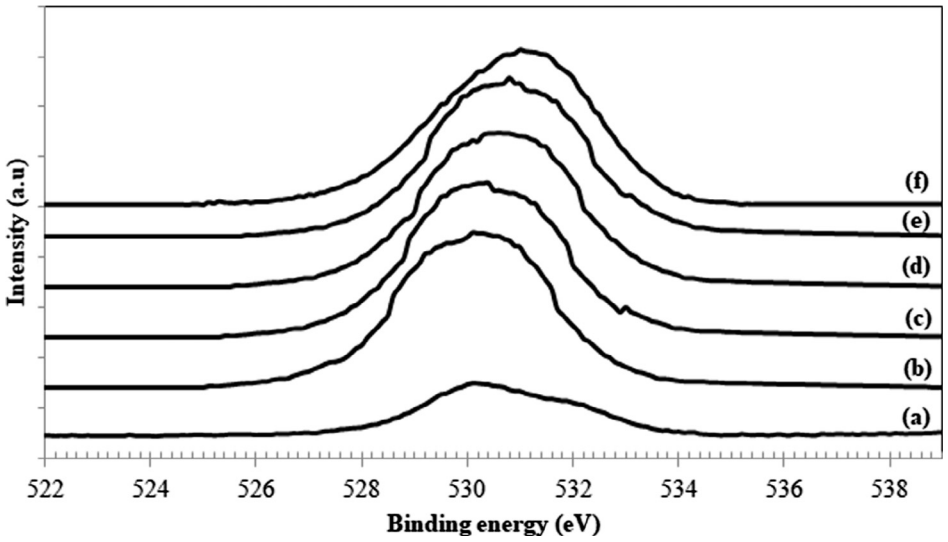


Fig. 3. XPS spectra of O1s for (a) pure ZrO_2, (b–e) pattern for modified forms (Mg:Zr 0.2–0.5) of base material MgO-ZrO_2 and (f) pure MgO.

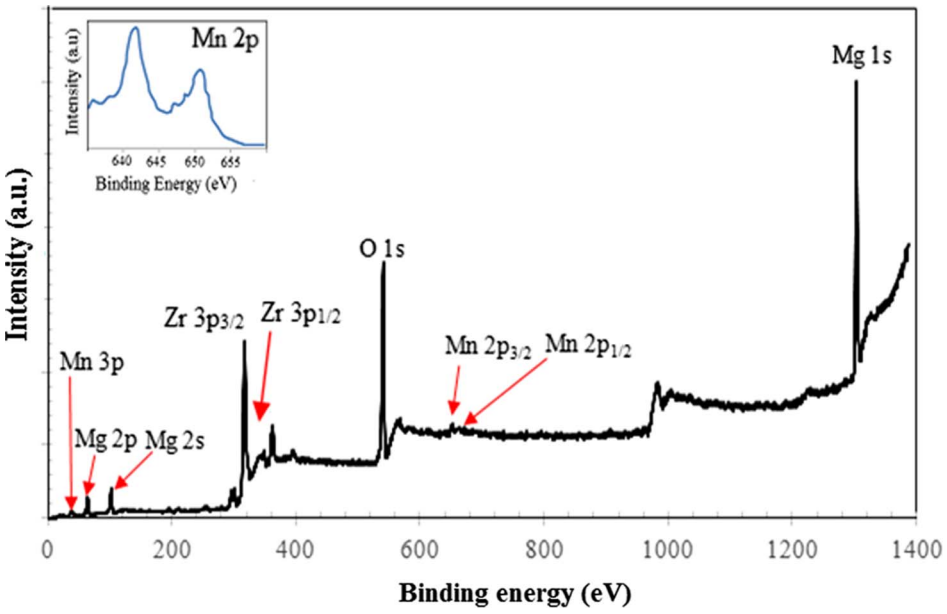


Fig. 4. XPS spectra of overall scan of Mn-MgO-ZrO_2 meanwhile high resolution insight image representing the presence of manganese (Mn $2p_{3/2}$ & $2p_{1/2}$).

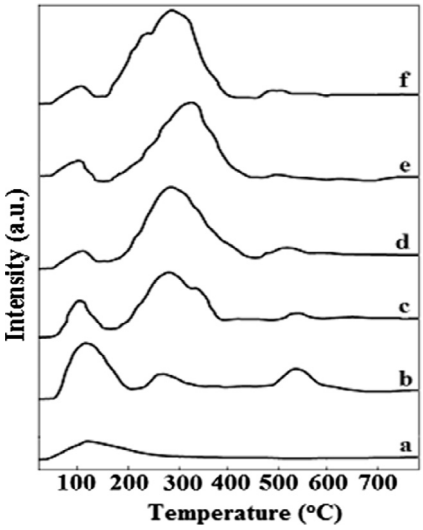


Fig. 5. CO_2-TPD profile for synthesized catalysts; (a) for pure ZrO_2 meanwhile pattern (b–e) for modified form of catalysts for 0.2–0.5 Mg:Zr and pattern (f) for Mn-Mg-ZrO_2 (0.4 Mg:Zr).

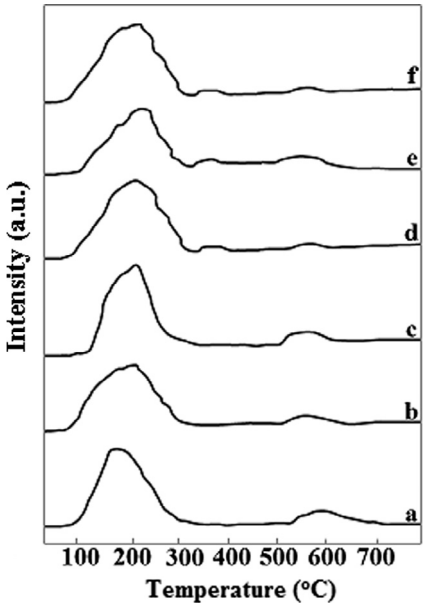


Fig. 6. NH_3-TPD profile for synthesized catalysts; (a) for pure ZrO_2 meanwhile pattern (b–e) for modified form of catalysts for 0.2–0.5 Mg:Zr and pattern (f) for Mn-Mg-ZrO_2 (0.4 Mg:Zr).

attributed to moderate and strong basic sites respectively [40].

So, it can be concluded that as the amount of MgO increased, the moderate basic sites increased, with redistribution of charges, which depends upon the structure of the material being synthesized. This can be related to physiochemical properties of catalysts, as it can be observed that as the quantity on MgO increases, the surface area and pore diameter increases. This might be due to the strong interaction between MgO-ZrO_2, which may lead to the generation of moderate basic sites when strong basic material MgO was mixed with ZrO_2. Similar kind of results has been reported earlier in, which Liu et al. observed that by increasing the MgO amount on ZrO_2, the strength of moderate sites increases [40]. Moreover, when Mn has been added to MgO-ZrO_2, the peak for moderate basic sites increases; further, the small shoulder peak was observed at 240 °C as shown in Fig. 5 (pattern f), which can be attributed to additional basic sites in the material. Moreover, the total amount of CO_2 adsorbed by Mn@0.4MgO-ZrO_2 mixed oxides was 3477.5 μmol/g.

NH_3-TPD is used to determine the acid sites present on the surface of catalysts, along with the total acid strength of the material by ammonia adsorption-desorption process. The acidic strength of synthesized catalysts has been shown in a NH_3-TPD pattern in Fig. 6. It can be noticed that pure ZrO_2 showed two different peaks, which refers to the presence of weak and strong basic sites. Moreover, when ZrO_2 was mixed with different amounts of MgO, it can be observed that it added up the weak acidic sites appearing between 130 and 300 °C, along with reduction of strong acidic sites (between 530 and 700 °C); and a small peak appears between 300 and 400 °C, which is ascribed to formation of moderate acidic sites. It has been reported that when basic oxides are mixed with zirconium oxide, the strong acidic sites are neutralized due to the presence of strong basic sites and generates weak and medium acidic sites [39]. However, for metallic oxide catalyst, by the addition of Mn, it can be observed from Fig. 6 (pattern f) that it adds up to weak and moderate strength active sites. Moreover, the total amount of NH_3 adsorbed by Mn@0.4MgO-ZrO_2 was 2123.2 μmol/g. So, it can be concluded that the synthesized catalysts possess both acidic and basic sites

Table 2
Physiochemical properties of synthesized catalysts.

Sample	Surface area S_A (m^2/g)	Pore Volume V_P (cm^3/g)	Pore Diameter D_P (nm)
ZrO_2	11.92	0.041	10.50
0.2 Mg:Zr	34.62	0.110	15.63
0.3 Mg:Zr	38.76	0.116	16.74
0.4 Mg:Zr	46.18	0.121	17.13
0.5 Mg:Zr	43.50	0.118	15.84
Mn0.4Mg:Zr	45.78	0.120	17.06

of different strengths. However, based on the amount of adsorbed gases (CO_2 and NH_3) it can be concluded that net charge is basic in character as the amount of CO_2 adsorbed is more than the amount of NH_3.

The physiochemical properties of synthesized catalysts which include surface area, pore volume and diameter are mentioned in Table 2. It can be observed that the parent ZrO_2 possesses a small surface area; however, when it is modified with MgO, the surface area is increased. The incremental surface area leads to the observation that there exist strong interactions in MgO and parent ZrO_2, which tend to increase surface diffusion of parent zirconia and cause a more stable crystal surface of the base material. Moreover, not only is the surface area increased, but pore volume and diameter are also increased, which might be due the strong interaction between the MgO and ZrO_2 (it can be observed from the higher binding energy shift in XPS analysis) leading to the formation of more uniform pore channels, which can allow efficient diffusion of reactant molecules within the catalyst. However, when the ratio of mixed oxides (Mg:Zr) was increased to 0.5 the surface area as well as pore size is reduced. This, decrement may to attributed to the fact that at high oxides ratio MgO doesn't interact with ZrO_2 and occupy the pores due which surface area, as well as pore size, was decreased. Due to which, catalyst performance can be affected. The average pore diameter of triglyceride molecule has been reported to be 5.8 nm and for efficient reaction for better yield, the pore structure of the catalyst should be tailored to support easy diffusion of reactant molecules [39]. The catalyst with big pore diameter along with hierarchal interconnected pore structure can allow better diffusion of reactant molecules, which allow greater interaction with active sites of catalyst and reveal efficient activity towards product formation. Meanwhile, when Mn was impregnated, the surface area decreased as well, but it was minor, leading to the observation that it was well dispersed and did not reduce the pore diameter as well while making more active sites available for reaction.

3.2. Catalyst evaluation

The activity of synthesized catalysts was evaluated for methanolysis of *Phoenix dactylifera* L. *kernel* oil for biodiesel production. First, the monometallic catalyst with MgO in different ratios doped with ZrO_2 was tested at fixed operating conditions such as temperature 65 °C, catalyst loading 4 wt%, methanol to oil molar ratio of 20:1 and reaction were carried out for 3 h. The trend of biodiesel yield by using different synthesized catalysts is shown in Fig. 7. It can be observed that as the amount of MgO is increased, the yield of biodiesel increases. MgO is known to be a highly basic material in nature and supports transesterification for biodiesel [30]. The high basic character of magnesium oxide is due to the presence of surface O^- ions, which help to capture the proton from the methanol, which tends to give the reactive species in the mixture. Meanwhile, Mg^{2+} ions present in lattice tend to give weak Lewis basic characteristics, which contribute to providing active sites for reaction [41]. So, methoxide species formed due to the basic character of the catalyst attack carbonyl carbons (nucleophilic sites) of the triglyceride molecules, to give biodiesel and glycerol as by-products [42].

It was observed that by increasing the amount of MgO on a support material, the basicity increased; however, from the physiochemical properties, it was revealed that surface area, as well as the pore diameter, increased, which allows easy adsorption of reactant molecules to the catalyst. Despite this, it is shown in Fig.7 that by increasing the MgO beyond a certain limit, the yield of biodiesel decreased. It has been reported earlier that strong basic material does not support efficient transesterification, as it may hold up the product molecules from desorbing, which tends to reduce the yield of biodiesel [43]. However, if referred to catalysts characterization also the basicity is increased by increasing MgO but due to the surface area of catalyst start decreasing which causes the upcoming MgO particles to block the pores and active sites which results in a decrement of biodiesel yield. As seen from CO_2-TPD, the strength of moderate basic sites increases while weak basic sites were very less, this revealed that the catalyst with moderate basic sites supports transesterification efficiently. Somehow, weak basic sites also tend to reduce the biodiesel yield by not allowing reactant molecules to adsorb the catalyst properly [43].

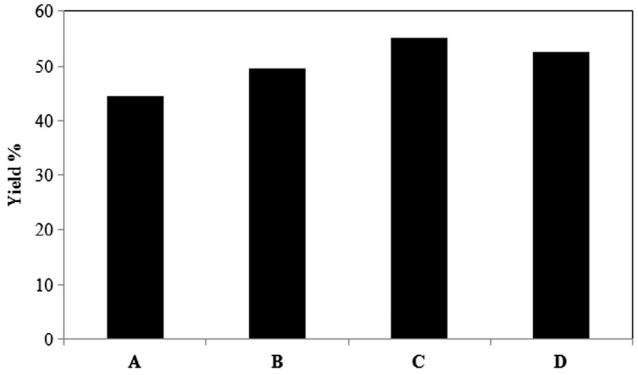


Fig. 7. Catalysts evaluation for biodiesel production through transesterification of waste *Phoenix dactylifera* L. kernel oil in presence of synthesized mixed oxides catalysts MgO-ZrO_2 (A = 0.2 (Mg:Zr); B = 0.3 (Mg:Zr); C = 0.4 (Mg:Zr) and D = 0.5 (Mg:Zr)).

So, it can be concluded that good performance of mixed oxides MgO-ZrO_2 (Mg:Zr = 0.4) can be related to the fact that it allows the optimal number of active sites for transesterification with efficient physiochemical properties. Therefore, in order to get a better catalyst, MgO-ZrO_2 (Mg:Zr = 0.4) mixed oxide support was further impregnated with transition metal (Mn 4 wt%) and observed that biodiesel yield was improved on similar operating conditions thus it can also be related to the characterization of the bimetallic catalyst. It can be observed that upon addition of Mn the surface area, as well as pore diameter, was not affected that much as shown in Table 1 which depicts it's well dispersed. Therefore, the metallic oxide catalyst was further studied for biodiesel synthesis and the process was optimized for operating conditions. The process variables selected for optimization include temperature, time, catalyst loading and methanol to oil molar ratio.

3.3. Parametric study for biodiesel production

Fig. 8 shows the parametric effect for biodiesel production while changing the process parameters. It can be observed that process temperature has a significant effect on the biodiesel yield. As the temperature is increased, the biodiesel increases up to 90 °C, which may be attributed to the fact that by increasing temperature, the viscosity of oil decreases and reactant molecules are in enough activation to transform into product diesel. However, it has been observed that increasing the temperature affinity of the carbonyl group of reactants increases towards the nucleophilic methanol and activation reaches the maximum, which enhances the product biodiesel yield. However, by increasing the temperature further, the yield of biodiesel is reduced. The decrement of yield at a higher temperature may be related to fact that lower amount of methanol becomes available for reaction due to the high rate of vaporization, which tends to reduce the yield of biodiesel. Moreover, it

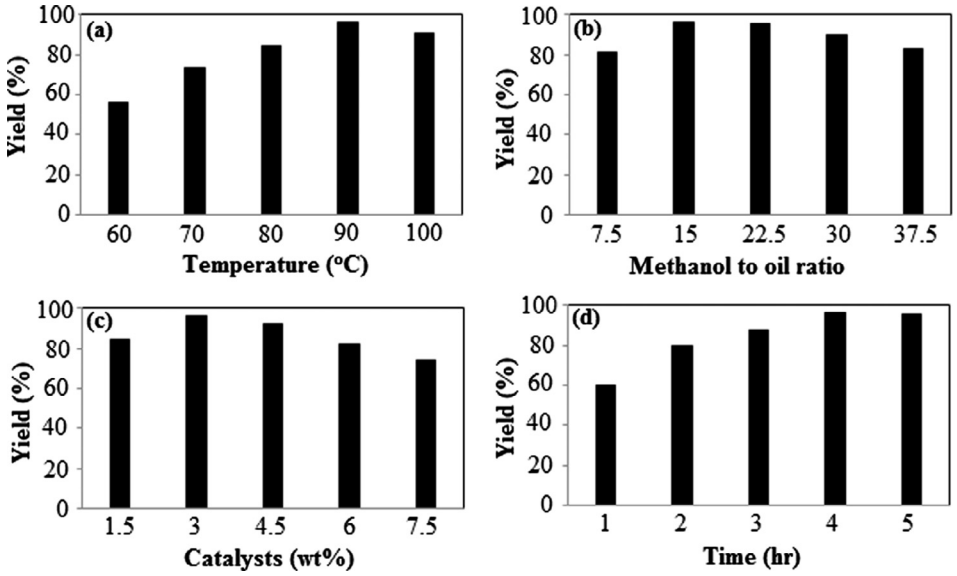


Fig. 8. Parametric study for biodiesel production (a) temperature, (b) methanol to oil ratio, (c) catalyst loading and (d) process time.

can be observed that initially, at low methanol to oil ratio, the yield of biodiesel is less, but tends to increase with an increase in the ratio; but after increasing it beyond 15, a slight decrement is observed in the yield and the same behavior continues by increasing the ratio further. This can be attributed to the fact that higher ratios may obstruct the by-product separation and tend to cause a reversible reaction. Process time plays an important role in biodiesel production; it can be observed that by increasing the time, the yield of biodiesel increases too, which can be attributed to the fact that by increasing the process, the interaction between reactants increases, which helps to increase the product yield. Moreover, this behavior of product yield towards process time is up to 4 h; if it is increased further, a slight decrement in yield was observed, which might be due to the reversible nature of the reaction, which caused it to move in the backward direction, due to excess process time [44]. The effect of catalyst loading on biodiesel yield depicts that up to 3 wt% of the catalyst possesses enough active sites, but by increasing it, the yield decreases. The decrement of yield might occur due to mass transfer issue and also due to excess amount of catalyst allowing more adsorption, which tends to reduce the yield. Thus, it can be concluded that synthesized catalyst gives high biodiesel production. Thus, based on the parametric study, the optimized set of conditions can be considered to be 90 °C temperature, methanol to oil ratio 15, process time 4 h and catalyst loading 3 wt%, which gave a 96.4% yield.

3.4. Catalyst reusability

Reusability of catalysts is an important aspect to be considered to upscale the process. The reusability of catalyst (Mn-MgO-ZrO_2) was determined on the optimal set of conditions such as temperature 90 °C, time 4 h, catalysts loading 3 wt% and methanol to oil ratio 15. Transesterification of oil was done repeatedly for six times; Fig. 9 shows the yield of biodiesel for each run. After each run, the catalyst was recovered, rinsed with methanol to remove all kind organic components (biodiesel, FFA and glycerol) which remained in it, dried thereafter in the oven at 100 °C for 5 h and finally, the dried sample was calcined at 650 °C for 4 h to activate the catalyst. This whole procedure was repeated after every run and metal compositions were also determined after each run.

The plot showing reusability of the catalyst depicts that the catalyst is highly active and can be reused several times, without any significant decrement in biodiesel yield. Based on the experimental data, the catalyst was highly active up to the fifth run, without any significant decrease; however, when it was used for the sixth time, the yield of

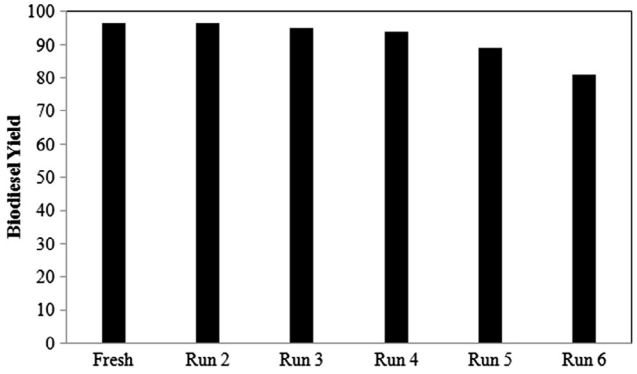


Fig. 9. Reusability of synthesized heterogeneous bimetallic catalyst for biodiesel production.

biodiesel was reduced significantly. Based on these results, it can observed that till the fourth run, the number of active sites was enough to give a good yield; however, in the last two runs, the decrement in yield may be attributed to the leaching of active metals or deposition of reactants on the catalyst surface. Moreover, the analysis of the used catalyst, by EDXS as shown in Table 3, revealed that the amount of active metal was not significantly affected till the fourth run; but after that, active metals were reduced. Further on, XRD patterns for fresh and used catalysts are shown in Fig. 10 and the only difference observed between both was a slight decrement in the intensity of peaks. Thus, the decrement in the peaks intensity may be attributed to the fact that it might be due to deposition of some amorphous material which is reaction material (oil, methanol or biodiesel). However, the crystallinity of the catalyst is sustained which can be attributed from the sharpness of peaks in the pattern of used catalyst. So, it can be concluded that the

Table 3
EDXS analysis of synthesized bimetallic heterogeneous catalyst for reusability in biodiesel production.

Catalyst	Mg (wt%)	Mn (wt%)
Fresh	34.90	3.60
2nd run	34.87	3.56
3rd run	34.83	3.49
4 th run	34.76	3.40
5 th run	34.55	3.25
6 th run	33.94	2.97

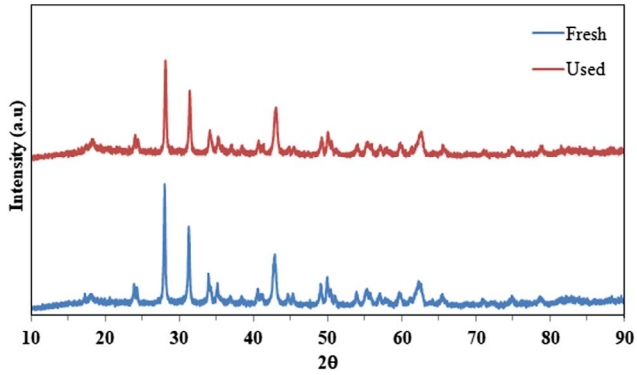


Fig. 10. XRD plot for fresh and used catalysts.

synthesized catalyst is highly active and reusable and can be considered for upscaling the process.

3.5. Reaction mechanism

In the present study, it proposed that for biodiesel production, both reactions-esterification and transesterification-occur simultaneously. To consider the occurrence of both reactions simultaneously, the catalyst should possess both acidic and basic active sites, as a characterization of catalysts revealed the presence of active sites with acidic and basic nature. ZrO_2 is amphoteric, possessing both acidic and basic active sites; and the strength of these sites is further increased by modifying with different metals such as magnesium and manganese oxides, which tends to increase the activity of the catalyst. The proposed mechanism is shown in Fig. 11, from which it can be seen as to how esterification proceeds due to the presence of acidic sites and transesterification due to basic sites, respectively.

A chemical reaction in the presence of heterogeneous catalyst involves three steps: adsorption of reactants on the catalyst, a chemical reaction between reactants on active sites and finally, desorption of products from the catalyst, as shown in Fig. 11. For biodiesel production, first, both reactants, triglyceride molecule and methanol get adsorbed of acidic and basic sites of catalyst respectively and changed to carbocation anoin from FFA molecule and oxygen anion from methanol. Then as a second step, a chemical reaction occurs as a nucleophilic attack of carbocation and oxygen anion on the hydroxyl group of methanol and carbonyl group of triglyceride for each present molecule, to support esterification and transesterification reactions respectively;

Table 4
Fuel properties of biodiesel produced from waste *Phoenix dactylifera* L. kernel oil.

Property	Present work	ASTM 6751	EN 14214
Acid value (mg KOH/g)	0.11	0.50 max	0.50 max
Density (kg/m^3) at 25 °C	881	–[a]	860–900
Kinematic viscosity (mm^2/s) at 40 °C	3.85	1.9–6.0	3.5–5.0
Flash point (°C)	142	93 min	120 min
Free glycerin (%)	0.011	0.020 max	0.020 max
Total glycerin (%)	0.162	0.240 max	0.250 max
Cetane number	61.12	47 min	51 min
Cloud point (°C)	3.69	Report	–[b]
Pour point (°C)	-1.23	–[a]	–[b]
Cold filter plugging point (°C)	-0.61	–[a]	–[b]
Calorific value (MJ/kg)	44.21	–[a]	–[a]

[a] Not specified.
[b] Not specified. EN 14214 uses time- and location-dependent values for the cold filter plugging point (CFPP) instead.

and due to this nucleophilic attack, tetrahedral intermediates are produced. Finally, bond breakage occurs of −OH and −C−O− and a hydroxyl group and alkyl triglycerides are desorbed respectively, which tends to give the final form known as monoalkyl ester (biodiesel) as a product. Meanwhile, active sites of the catalyst become available for another reaction cycle and this continues depending on the required time for reaction completion. Hence, during this reaction, water and glycerol are obtained as byproducts.

3.6. Quality analysis of biodiesel

In order to evaluate the quality of biodiesel so as to run it in the conventional diesel engine in replacement of fossil diesel, it should meet the international standards set by the American Society for Testing Material (ASTM) and European standards (EN). A number of tests have been conducted to evaluate the quality of biodiesel synthesized from *Phoenix dactylifera* L. kernel oil and the measured values of tests, along with the comparison to values mentioned by ASTM 6751 and EN 14214, are shown in Table 4. The acid value of biodiesel synthesized is 0.11 and this lies within the range defined by international standards, which indicates that acidic content in biodiesel has been reduced to a large extent and formed methyl ester of acids are present in the oil. The density of synthesized biodiesel is 881 kg/m and it lies within the range defined for density by the EN14214 standard. The density of biodiesel can affect the engine performance, as it has a significant influence on the break-up of fuel when injected. The viscosity

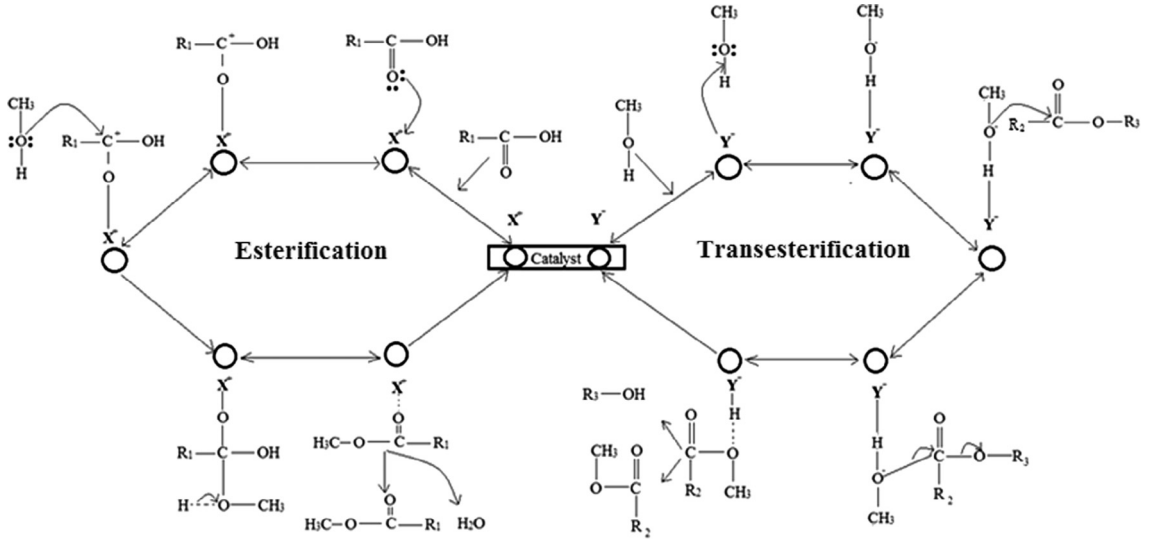


Fig. 11. Proposed reaction mechanism of biodiesel production in presence of synthesized bimetallic catalyst.

Table 5
Economical comparison of biodiesel produced from waste *Phoenix dactylifera* L. kernel oil with conventionally produced biodiesel from different edible and non-edible oils.

Feedstock	Catalyst	Cost (US $/L)	Reference
Waste *Phoenix dactylifera* L. kernel oil	Mn@MgO-ZrO_2	0.46	Present work
Palm oil	NaOH	2.30	[48]
Waste cooking oil	KOH	0.58	[49]
Sunflower oil	KOH	0.99	[50]
Jatropha oil	CaO	0.66	[51]

of produced biodiesel was measured to be 3.85 mm^2/s, which is within the range defined by standards for suitable biodiesel for better combustion in the engine. The viscosity of fuel has a large impact on its combustion, as it can cause a problem in fuel atomization, due to which engine efficiency decreases. The viscosity of fuel depends on carbon chain length and high viscosity reflects the presence of unreacted long chain components, similar to those present in source oil. Flashpoint measured for synthesized biodiesel was 142 °C and it satisfies the international standards. It is the minimum temperature at which vapours of fuel can be easily ignited. Determining the flash point of biodiesel is important, as it can affect the storage and transportation of biodiesel. Measured values for free and total glycerin were 0.011 and 0.162, which were less than the maximum limit defined ASTM and EN. As glycerin is a by-product of reaction in the production of biodiesel from triglycerides by transesterification, this is a reversible reaction and if it is not separated from the product, it can increase the acid value and decrease the yield of biodiesel. So, the amount of glycerin should be reduced as much as possible from the product, to increase the storage stability of biodiesel. The cetane number of the produced biodiesel is 61.12 and it satisfies the limit defined by international standards. The cetane number of biodiesel is an important parameter to be determined, as it affects the engine performance directly. It is an anti-knocking property and is higher for biodiesel derived from oil with a high percentage of saturated fatty acids. Cold flow properties determined for biodiesel which includes cloud point, pour point and cold filter plugging point, are 3.69, −1.23 and −0.61 °C and for these, there are not defined ranges as such for biodiesel. The calorific value measure for produced biodiesel is 44.21 MJ/kg and is quite comparable to fossil diesel. It is an important property with reference to energy density possessed by biodiesel and it is necessary to calculate a calorific value for measuring the engine thermal efficiency when operating on the test fuel. Despite all positive aspects, there are few limitations for biodiesel to be used as a fuel when compared to fossil diesel which includes; poor low-temperature operability if biodiesel exposed to open atmosphere it can attract moisture which affects the stability and biodiesel can cause a reduction in fuel economy. However, low-temperature operability can be overcome by using green additive produced from bio-glycerol which is obtained as a by-product from transesterification [45].

4. Economical analysis

Economic feasibility is considered to be the major factor influencing the sustainability of biodiesel to be used as a fuel. The main factor influencing the economic viability of biodiesel is the type of feedstock utilized to produce biodiesel which accounts 70–95% of overall biodiesel cost [46,47]. Thus, in current research work, the biodiesel is produced from waste *Phoenix dactylifera* L. kernels which were obtained free of cost. Waste *Phoenix dactylifera* L. kernels are non-edible and if used to produce biodiesel can help in handling the solid waste management [9]. Moreover, another factor which adds up to biodiesel production is nature of the catalyst. The catalyst can be either homogeneous or heterogeneous, in most of the commercial plant's conventional homogeneous catalysts (NaOH and KOH) are used which are non-recoverable from the process and are not reusable, thus cause to increase the biodiesel cost. However, if efficient heterogeneous catalysts are used for biodiesel production can help to reduce the overall biodiesel cost by 5–10% [20]. Thus, in the current process, efficient heterogeneous catalyst (Mn@MgO-ZrO_2) is synthesized which gave 96.4% yield and reused for up to six repeated reaction cycles. The cost analysis revealed that biodiesel is produced at 0.46 US $/L on lab scale. However, the cost of biodiesel is quite better and comparable to conventionally used oils for biodiesel production as mentioned in Table 5. It can be seen that cost of produced biodiesel is less as compared to biodiesel produced from edible oils (Palm oil and Sunflower oil) and non-edible oils (waste cooking oil and Jatropha oil). Thus, it can be concluded that biodiesel produced from waste *Phoenix dactylifera* L. kernel powder in presence of efficient heterogeneous catalyst is cost effective and based on its fuel properties it has potential to be used as fuel.

5. Conclusions

The metallic oxide catalyst was successfully synthesized by a modified route which involves co-precipitation and incipient impregnation. The characterization results revealed that in synthesized metallic oxide catalyst, a combination of oxides and chemical environment played an important role. Thus, the synthesized catalyst was with better physiochemical chemical properties, which opened the interface for better transesterification reaction to give a high biodiesel yield. The metallic oxide catalyst (Mn-MgO-ZrO_2) was used for optimizing the biodiesel production, which revealed the maximum yield obtained to be 96.4% with the following operating variables; temperature 90 °C, time 4 h, catalyst loading 3 wt% and methanol to oil ratio 15:1. The efficient catalytic activity of the synthesized catalyst can be related to its properties such as balanced active sites and better structure with proper pore size. The characterization of produced biodiesel revealed that it possesses fuel properties which satisfy the international standards defined by ASTM and EN. Thus, it can be concluded that the synthesized catalyst is highly efficient and the biodiesel produced can be used as a potential source for transportation, based on its fuel properties.

Acknowledgement

The authors would like to thank The Research Council of Oman for its financial support under grant number ORG/EI/13/013.

Appendix A. Supplementary material

Supplementary data associated with this article can be found, in the online version, at http://dx.doi.org/10.1016/j.enconman.2017.10.064.

References

[1] Mofijur M, Masjuki HH, Kalam MA, Atabani AE, Shahabuddin M, Palash SM, et al. Effect of biodiesel from various feedstocks on combustion characteristics, engine durability and materials compatibility: a review. Renew Sustain Energy Rev 2013;28:441–55.
[2] Banković-Ilić IB, Stamenković OS, Veljković VB. Biodiesel production from non-edible plant oils. Renew Sustain Energy Rev 2012;16:3621–47.
[3] Sajjadi B, Raman AAA, Arandiyan H. A comprehensive review on properties of edible and non-edible vegetable oil-based biodiesel: composition, specifications and prediction models. Renew Sustain Energy Rev 2016;63:62–92.
[4] Moser BR. Biodiesel production, properties, and feedstocks. Vitro Cell Dev Biol – Plant 2009;45:229–66.
[5] Hernández B, Martín M. Optimal Integrated Plant for Production of Biodiesel from waste. ACS Sustain Chem Eng 2017.
[6] Manickavasagan A, Essa MM, Sukumar E. Dates production, processing, food and medical values. New York: CRC Press; 2012.
[7] Al-Muhtaseb AAH, Jamil F, Al-Haj L, Al-Hinai MA, Baawain M, Myint MTZ, et al. Efficient utilization of waste date pits for the synthesis of green diesel and jet fuel fractions. Energy Convers Manage 2016;127:226–32.
[8] Amani MA, Davoudi MS, Tahvildari K, Nabavi SM, Davoudi MS. Biodiesel production from Phoenix dactylifera as a new feedstock. Ind Crops Prod 2013;43:40–3.

[9] Jamil F, Al-Muhtaseb AAH, Al-Haj L, Al-Hinai MA, Hellier P, Rashid U. Optimization of oil extraction from waste "Date pits" for biodiesel production. Energy Convers Manage 2016;117:264–72.
[10] Nehdi I, Omri S, Khalil MI, Al-Resayes SI. Characteristics and chemical composition of date palm (Phoenix canariensis) seeds and seed oil. Ind Crops Prod 2010;32:360–5.
[11] Al-Farsi MA, Lee CY. Optimization of phenolics and dietary fibre extraction from date seeds. Food Chem 2008;108:977–85.
[12] Al-Farsi M, Alasalvar C, Al-Abid M, Al-Shoaily K, Al-Amry M, Al-Rawahy F. Compositional and functional characteristics of dates, syrups, and their by-products. Food Chem 2007;104:943–7.
[13] Azeem MW, Hanif MA, Al-Sabahi JN, Khan AA, Naz S, Ijaz A. Production of biodiesel from low priced, renewable and abundant date seed oil. Renewable Energy 2016;86:124–32.
[14] Knothe G. 1 – Introduction. The biodiesel handbook, 2nd ed. AOCS Press; 2010. p. 1–3.
[15] Aransiola EF, Ojumu TV, Oyekola OO, Madzimbamuto TF, Ikhu-Omoregbe DIO. A review of current technology for biodiesel production: state of the art. Biomass Bioenerg 2014;61:276–97.
[16] Knothe G, Razon LF. Biodiesel fuels. Prog Energy Combust Sci 2017;58:36–59.
[17] Al-Sakkari EG, El-Sheltawy ST, Attia NK, Mostafa SR. Kinetic study of soybean oil methanolysis using cement kiln dust as a heterogeneous catalyst for biodiesel production. Appl Catal B 2017;206:146–57.
[18] Li J, Guo Z. Structure evolution of synthetic amino acids-derived basic ionic liquids for catalytic production of biodiesel. ACS Sustain Chem Eng 2017;5:1237–47.
[19] Boffito DC, Mansi S, Leveque JM, Pirola C, Bianchi CL, Patience GS. Ultrafast biodiesel production using ultrasound in batch and continuous reactors. ACS Sustain Chem Eng 2013;1:1432–9.
[20] Anuar MR, Abdullah AZ. Challenges in biodiesel industry with regards to feedstock, environmental, social and sustainability issues: a critical review. Renew Sustain Energy Rev 2016;58:208–23.
[21] Chouhan APS, Sarma AK. Modern heterogeneous catalysts for biodiesel production: a comprehensive review. Renew Sustain Energy Rev 2011;15:4378–99.
[22] de Lima AL, Ronconi CM, Mota CJA. Heterogeneous basic catalysts for biodiesel production. Catal Sci Technol 2016;6:2877–91.
[23] Liang X, Gao S, Wu H, Yang J. Highly efficient procedure for the synthesis of biodiesel from soybean oil. Fuel Process Technol 2009;90:701–4.
[24] Liang X, Gao S, Yang J, He M. Highly efficient procedure for the transesterification of vegetable oil. Renewable Energy 2009;34:2215–7.
[25] Zhang F, Fang Z, Wang Y-T. Biodiesel production direct from high acid value oil with a novel magnetic carbonaceous acid. Appl Energy 2015;155:637–47.
[26] Chang F, Zhou Q, Pan H, Liu X-F, Zhang H, Xue W, et al. Solid mixed-metal-oxide catalysts for biodiesel production: a review. Energy Technol 2014;2:865–73.
[27] Su F, Guo Y. Advancements in solid acid catalysts for biodiesel production. Green Chem 2014;16:2934–57.
[28] Suresh R, Antony JV, Vengalil R, Kochimoolayil GE, Joseph R. Esterification of free fatty acids in non- edible oils using partially sulfonated polystyrene for biodiesel feedstock. Ind Crops Prod 2017;95:66–74.
[29] Chai M, Tu Q, Lu M, Yang YJ. Esterification pretreatment of free fatty acid in biodiesel production, from laboratory to industry. Fuel Process Technol 2014;125:106–13.
[30] Farooq M, Ramli A, Subbarao D. Biodiesel production from waste cooking oil using bifunctional heterogeneous solid catalysts. J Clean Prod 2013;59:131–40.
[31] Alhassan FH, Rashid U, Taufiq-Yap YH. Synthesis of waste cooking oil-based biodiesel via effectual recyclable bi-functional $Fe_2O_3MnOSO_{42}^{-}/ZrO_2$ nanoparticle solid catalyst. Fuel 2015;142:38–45.
[32] Li H, Fang Z, Smith Jr. RL, Yang S. Efficient valorization of biomass to biofuels with bifunctional solid catalytic materials. Prog Energy Combust Sci 2016;55:98–194.
[33] Raia RZ, da Silva LS, Marcucci SMP, Arroyo PA. Biodiesel production from Jatropha curcas L. oil by simultaneous esterification and transesterification using sulphated zirconia. Catal Today; 2017.
[34] Zhang Y, Wong W-T, Yung K-F. One-step production of biodiesel from rice bran oil catalyzed by chlorosulfonic acid modified zirconia via simultaneous esterification and transesterification. Biores Technol 2013;147:59–64.
[35] Renuka L, Anantharaju KS, Sharma SC, Nagaswarupa HP, Prashantha SC, Nagabhushana H, et al. Hollow microspheres Mg-doped ZrO_2 nanoparticles: Green assisted synthesis and applications in photocatalysis and photoluminescence. J Alloys Compd 2016;672:609–22.
[36] García V, Fernández JJ, Ruíz W, Mondragón F, Moreno A. Effect of MgO addition on the basicity of Ni/ZrO_2 and on its catalytic activity in carbon dioxide reforming of methane. Catal Commun 2009;11:240–6.
[37] Lee JK, Lee H, Hong UG, Lee J, Cho Y-J, Yoo Y, et al. Oxidative dehydrogenation of n-butane to n-butene and 1,3-butadiene over $Mg_3(VO_4)_2/MgO–ZrO_2$ catalysts: Effect of Mg: Zr ratio of support. J Ind Eng Chem 2012;18:1096–101.
[38] Wang J-G, Yang Y, Huang Z-H, Kang F. Rational synthesis of MnO_2/conducting polypyrrole@carbon nanofiber triaxial nano-cables for high-performance supercapacitors. J Mater Chem 2012;22:16943–9.
[39] Wan Omar WNN, Amin NAS. Biodiesel production from waste cooking oil over alkaline modified zirconia catalyst. Fuel Process Technol 2011;92:2397–405.
[40] Liu S, Zhang X, Li J, Zhao N, Wei W, Sun Y. Preparation and application of stabilized mesoporous $MgO–ZrO_2$ solid base. Catal Commun 2008;9:1527–32.
[41] Lu F, Yu W, Yu X, Tu S-T. Transesterification of vegetable oil to biodiesel over $MgO-Li_2O$ catalysts templated by a PDMS-PEO comb-like copolymer. Energy Procedia 2015;75:72–7.
[42] Islam A, Taufiq-Yap YH, Chu C-M, Chan E-S, Ravindra P. Studies on design of heterogeneous catalysts for biodiesel production. Process Saf Environ Prot 2013;91:131–44.
[43] Kannan DC. A solid catalyst method for biodiesel production. Pennsylvania State University; 2009.
[44] Wan L, Liu H, Skala D. Biodiesel production from soybean oil in subcritical methanol using $MnCO_3$/ZnO as catalyst. Appl Catal B 2014;152–153:352–9.
[45] Jamil F, Saxena SK, Al-Muhtaseb AAH, Baawain M, Al-Abri M, Viswanadham N, et al. Valorization of waste "date seeds" bio-glycerol for synthesizing oxidative green fuel additive. J Clean Prod 2017;165:1090–6.
[46] Sajid Z, Zhang Y, Khan F. Process design and probabilistic economic risk analysis of bio-diesel production. Sustain Prod Consump 2016;5:1–15.
[47] Lee S, Posarac D, Ellis N. Process simulation and economic analysis of biodiesel production processes using fresh and waste vegetable oil and supercritical methanol. Chem Eng Res Des 2011;89:2626–42.
[48] Jegannathan KR, Eng-Seng C, Ravindra P. Economic assessment of biodiesel production: comparison of alkali and biocatalyst processes. Renew Sustain Energy Rev 2011;15:745–51.
[49] Sakai T, Kawashima A, Koshikawa T. Economic assessment of batch biodiesel production processes using homogeneous and heterogeneous alkali catalysts. Biores Technol 2009;100:3268–76.
[50] Tasić MB, Stamenković OS, Veljković VB. Cost analysis of simulated base-catalyzed biodiesel production processes. Energy Convers Manage 2014;84:405–13.
[51] Labib TM, Hawash SI, El-Khatib KM, Sharaky AM, El Diwani GI, Abdel Kader E. Kinetic study and techno-economic indicators for base catalyzed transesterification of Jatropha oil. Egypt J Petrol 2013;22:9–16.